

## Electronic Structure of Strongly Correlated $d$ -Wave Superconductors

Bernhard Edegger,<sup>1,2,3</sup> V. N. Muthukumar,<sup>2</sup> Claudius Gros,<sup>1</sup> and P. W. Anderson<sup>3</sup>

<sup>1</sup>*Institute for Theoretical Physics, Universität Frankfurt, D-60438 Frankfurt, Germany*

<sup>2</sup>*Department of Physics, City College of the City University of New York, New York, New York 10031, USA*

<sup>3</sup>*Department of Physics, Princeton University, Princeton, New Jersey 08544, USA*

(Received 25 December 2005; published 24 May 2006)

We study the electronic structure of a strongly correlated  $d$ -wave superconducting state. Combining a renormalized mean field theory with direct calculation of matrix elements, we obtain explicit analytical results for the nodal Fermi velocity  $v_F$ , the Fermi wave vector  $k_F$ , and the momentum distribution  $n_k$  as a function of hole doping in a Gutzwiller projected  $d$ -wave superconductor. We calculate the energy dispersion  $E_k$  and spectral weight of the Gutzwiller-Bogoliubov quasiparticles and find that the spectral weight associated with the quasiparticle excitation at the antinodal point shows a nonmonotonic behavior as a function of doping. Results are compared to angle resolved photoemission spectroscopy of the high-temperature superconductors.

DOI: 10.1103/PhysRevLett.96.207002

PACS numbers: 74.20.Mn, 71.10.Fd, 71.10.Li

Recent progress in angle resolved photoemission spectroscopy (ARPES) of the high-temperature superconductors has led to considerable interest in the electronic structure of a strongly correlated  $d$ -wave superconducting state [1,2]. Experiments show a variety of interesting phenomena, and it is generally agreed that strong electronic correlations play a dominant role in explaining some of the universal spectral features. Hence, it would be desirable to obtain, e.g., for comparison with experimental results, explicit analytical results from a simple model of a strongly correlated  $d$ -wave superconductor.

Thus motivated, we consider in this Letter the electronic structure of a Gutzwiller projected superconductor, defined by the ground state wave function  $\exp(iS)|\Psi\rangle \equiv \exp(iS)P_G|\Psi_0\rangle$ . The projection operator  $P_G \equiv \prod_i (1 - n_{i\uparrow}n_{i\downarrow})$ , acting on a BCS wave function  $|\Psi_0\rangle$ , eliminates states with double occupancies in  $|\Psi\rangle$ . The operator  $\exp(iS)$  allows for a systematic calculation of corrections to the fully projected state  $|\Psi\rangle$  [3,4]. Gutzwiller projected states  $|\Psi\rangle$  were initially proposed as variational states to describe superconductivity in the proximity of a Mott insulating phase [5–7]. They have been used recently for numerical investigations of the electronic structure of the high-temperature superconductors. Paramekanti *et al.* used a variational Monte Carlo (VMC) technique to study some spectral properties of a Gutzwiller projected  $d$ -wave superconductor [3]. Yunoki *et al.* extended the VMC technique to the direct calculation of excited states in Jastrow-Gutzwiller wave functions [8]. The VMC technique also allows one to study the coexistence of superconductivity with antiferromagnetism [9] and the quasiparticle current renormalization [10].

In this Letter, we will follow an alternate route and use a combination of renormalized mean field theory (RMFT) [7] and direct calculation of matrix elements [4,11] to examine the electronic structure of a Gutzwiller projected  $d$ -wave superconductor. Though Gutzwiller projection is only an approximate method to treat the effects of strong

correlations, the advantage lies in its directness and clarity. Explicit analytical expressions derived in this Letter can be used to evaluate directly the successes as well as the limitations of this approach. Using RMFT, we determine the energy dispersion  $E_k$  of the Gutzwiller-Bogoliubov quasiparticles and the nodal Fermi velocity  $v_F$ . We show that  $v_F$  stays finite as the (Mott) insulating phase is approached. We calculate the spectral weight associated with the  $d$ -wave quasiparticles and the momentum distribution  $n_k$  by a direct evaluation of the relevant matrix elements [11]. We find that the quasiparticle weight associated with the antinodal excitation exhibits a nonmonotonic behavior as a function of doping.

We consider the one band Hubbard model

$$H = - \sum_{\langle ij \rangle, \sigma} t_{ij} (c_{i\sigma}^\dagger c_{j\sigma} + c_{j\sigma}^\dagger c_{i\sigma}) + U \sum_i n_{i\uparrow} n_{i\downarrow},$$

where the hopping integrals  $t_{ij}$  connect sites  $i$  and  $j$ . We will restrict our attention to nearest ( $t$ ) and next nearest ( $t' = -t/4$ ) neighbor hopping. We choose an on-site repulsion  $U = 12t$ ; i.e., we work in the strong coupling regime  $U \gg t, t'$  [12]. In this limit, a unitary transformation  $\exp(iS)$  yields an effective Hamiltonian  $H_{\text{eff}} = \exp(-iS)H\exp(iS)$ , which is block diagonal and does not mix states between the lower and upper Hubbard bands [3,13]. To  $\mathcal{O}(t^2/U)$ , it corresponds to the  $t - J$  Hamiltonian with the correlated hopping term (three-site term), for which the Gutzwiller wave function  $P_G|\Psi_0\rangle$  has been established as an excellent variational ground state [6]. Retransformation of the trial wave function  $\exp(iS)P_G|\Psi_0\rangle$  then provides a systematic way to study the Hubbard model using Gutzwiller projected states.

Two steps are necessary to obtain explicit analytic expressions for the low energy properties in the strong coupling regime. The first is the Gutzwiller renormalization procedure, where the effects of the projection  $P_G$  are taken into account by appropriate renormalization factors,

following Hilbert space counting arguments:  $\langle \Psi_0 | P_G H_{\text{eff}} P_G | \Psi_0 \rangle \approx \langle \Psi_0 | \tilde{H}_{\text{eff}} | \Psi_0 \rangle$  [7,14,15].

The next step is the realization that  $\tilde{H}_{\text{eff}}$  allows for two types of molecular fields: the hopping amplitude  $\xi_r \equiv \sum_{\sigma} \langle c_{i\sigma}^{\dagger} c_{i+r\sigma} \rangle_0$  and the singlet pairing amplitude  $\Delta_r \equiv \langle c_{i1}^{\dagger} c_{i+r1}^{\dagger} - c_{i1}^{\dagger} c_{i+r1}^{\dagger} \rangle_0$ , where  $r$  connects nearest (NN) or next nearest neighboring (NNN) sites;  $\langle \dots \rangle_0$  denotes the expectation value with respect to  $|\Psi_0\rangle$ .

This decoupling scheme of the renormalized Hamiltonian (RMFT) leads to a BCS ground state  $|\Psi_0\rangle = \prod_k (u_k + v_k c_{k1}^{\dagger} c_{-k1}^{\dagger}) |0\rangle$ , with  $v_k^2 = (1 - \zeta_k/E_k)/2$  and  $u_k^2 = 1 - v_k^2$ . The corresponding gap equations are  $\xi_r = -(1/L) \times \sum_k \cos(kr) \zeta_k/E_k$  and  $\Delta_r = (1/L) \sum_k \cos(kr) \tilde{\Delta}_k/E_k$ , together with the condition  $x = (1/L) \sum_k \zeta_k/E_k$  for the hole-doping concentration [7,16].

Solving the gap equations, we find that a  $d$ -wave pairing state is most stable for  $x \leq 0.4$ . In this case,  $\Delta \equiv |\Delta_x| = |\Delta_y|$ , with  $\Delta_x = -\Delta_y$ ,  $\xi \equiv \xi_x = \xi_y$ , and  $\xi' \equiv \xi_{x+y} = \xi_{x-y}$ . The dispersion relation of the Gutzwiller-Bogoliubov quasiparticle is given by  $E_k = \sqrt{\zeta_k^2 + \Delta_k^2}$ , where

$$\begin{aligned} \zeta_k = & - \left( 2g_t t + J \frac{\xi}{4} x_1 + J' \frac{\xi'}{4} x_2 \right) (\cos k_x + \cos k_y) \\ & - \left( 2g_t t' + J'' \frac{\xi'}{4} x_1 + J' \frac{\xi}{4} x_2 \right) 2 \cos k_x \cos k_y \\ & - x_D \sum_{\tau \neq \tau'} \frac{t_{\tau} t_{\tau'}}{4U} \cos[k(\tau - \tau')] - \mu, \end{aligned} \quad (1)$$

$$\tilde{\Delta}_k = J \frac{\Delta}{4} [3g_s + 1 - (3+x)g_3] (\cos k_x - \cos k_y). \quad (2)$$

In Eqs. (1) and (2), the Gutzwiller factors corresponding to the kinetic, superexchange, and the three-site terms are  $g_t = 2x/(1+x)$ ,  $g_s = 4/(1+x)^2$ , and  $g_3 = 4x/(1+x)^2$ , respectively [14]. The last sum in Eq. (1) is a sum over all pairs of neighboring sites  $\tau$  and  $\tau'$ , where  $t_{\tau}$  and  $t_{\tau'}$  are the NN and NNN hopping terms, respectively. We define  $J = 4t^2/U$ ,  $J' = 4t't/U$ , and  $J'' = 4t'^2/U$  and abbreviate  $x_1 = 3g_s - 1 + 3(3-x)g_3$ ,  $x_2 = 4(3-x)g_3$ , and  $x_D = (1-x^2)g_3$  in Eq. (1).

Figure 1(a) shows the doping dependence of the mean field hopping parameters  $\xi$  and  $\xi'$  and the  $d$ -wave mean field pairing  $\Delta$ , obtained by solving the RMFT gap equations. Since  $g_t$ ,  $g_3$ ,  $x_2$ ,  $x_D$ , and  $\xi'$  vanish as  $x \rightarrow 0$ , the dispersion relation  $\zeta_k \rightarrow -(11/4)J\xi(\cos k_x + \cos k_y)$  in the limit of zero doping.

The  $d$ -wave order parameter  $\Delta$  decreases nearly linearly with doping and vanishes around  $x \approx 0.4$ , for our choice of parameters. This is in agreement with previous studies [7,17]. Note that we retain *all* terms of  $\mathcal{O}(t^2/U)$  in the effective Hamiltonian  $H_{\text{eff}}$ , including the three-site term, which suppresses  $d$ -wave pairing in the overdoped regime.

The doping dependence of the superconducting (SC) gap  $|\tilde{\Delta}_k|$  at  $k = (\pi, 0)$  is shown in Fig. 1(b). The doping dependence resembles experimental observations quite

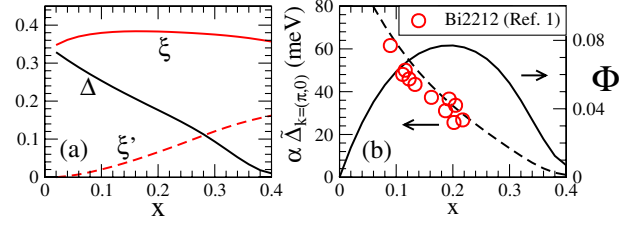


FIG. 1 (color online). (a) Doping dependence of the dimensionless mean field parameters  $\xi$ ,  $\xi'$ ,  $\Delta$ ; (b) doping dependence of (solid line) the SC order parameter  $\Phi$  and (dashed line) the SC gap  $\alpha|\tilde{\Delta}_k|$ , at  $k = (\pi, 0)$  for  $t = 300$  meV. The RMFT SC gap is scaled by a factor  $\alpha = 1/2$  for comparison with experimental data (red circles, Bi2212 [1]).

well. However, the gap is overestimated by a factor of about 2 [see scaling factor  $\alpha = 1/2$  in Fig. 1(b)] within mean field theory, which neglects additional off-site correlations as well as dynamical effects due to the motion of holes [18]. The SC gap is not identical to the true SC order parameter  $\Phi \equiv |\langle c_{i1}^{\dagger} c_{i+\tau 1}^{\dagger} - c_{i1}^{\dagger} c_{i+\tau 1}^{\dagger} \rangle|$  [3,7]. Here  $\tau$  is a neighboring site and  $\langle \dots \rangle$  represents the expectation value calculated with the retransformed wave function  $\exp(iS)P_G|\Psi_0\rangle$ . Calculating  $\Phi$  to  $\mathcal{O}(t/U)$ , we find  $\Phi \approx g_t \Delta + (t/U)g_3(6-x)\Delta\xi$ , where we set  $t' \approx 0$  for simplicity. As shown in Fig. 1(b),  $\Phi$  vanishes as  $x \rightarrow 0$ , as it should.

We now consider the nature of the low lying excitations, the quasiparticles created at the nodal point  $k_F$ . The nodal dispersion around  $k_F$  is characterized by the velocity  $v_F$ , which directly influences a number of experimentally accessible quantities. Within RMFT,  $v_F$  is directly obtained by calculating the gradient of  $\zeta_k$  along the direction  $(0, 0) \rightarrow (\pi, \pi)$ . The result is presented in Fig. 2(a) (for  $t = 0.3, 0.4, 0.5$  eV and  $a_0 = 4$  Å) and is well approximated by the formula

$$v_F/a_0 \approx \sqrt{2} \sin k_F \left[ 2g_t(t + 2t' \cos k_F) + x_1 \frac{J}{4} \xi \right]. \quad (3)$$

In the above equation, we set  $J'$ ,  $J''$ , and  $x_D$  to zero for simplicity. As seen in Fig. 2,  $v_F$  increases with  $x$  but remains finite as  $x \rightarrow 0$ . As can be inferred from Eq. (3),

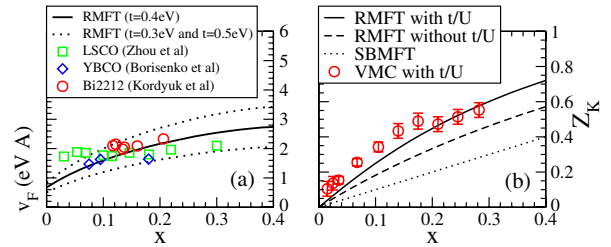


FIG. 2 (color online). Doping dependence of (a) Fermi velocity  $v_F$  and (b) renormalization  $Z_k$  of the Gutzwiller-Bogoliubov nodal quasiparticle. RMFT results are compared with experiments [in (a), data from Ref. [19]] and VMC [in (b), data from Ref. [3]], respectively.

the energy scale of the nodal velocity at  $x = 0$  is determined by  $J$ ; i.e.,  $v_F/(a_0J) \approx \sqrt{2} \sin(k_F) \frac{1}{4} \xi \approx 1.5$  (for  $\xi \approx 0.38$  and  $k_F \approx \frac{\pi}{2}$ ). The observed doping dependence stems from the effects of Gutzwiller projection  $P_G$ . As  $x$  increases, holes gain kinetic energy by direct hopping, viz.,  $g_t$  increases with doping, but  $g_s$  decreases, leading to the doping dependence of  $v_F$  seen in Fig. 2.

Our results agree with the numerical VMC results of Paramekanti *et al.*, who extract  $v_F$  from the discontinuity of the first moment of the spectral function in the repulsive  $U$  Hubbard model [3], and those of Yunoki *et al.*, who obtain  $v_F$  from the quasiparticle dispersion in the  $t - J$  model [8]. A comparison to ARPES data [19], presented in Fig. 2(a), shows good agreement. The doping dependence of  $v_F$  in the severely underdoped regime remains to be settled experimentally. While some groups report a nearly constant Fermi velocity [see data for  $\text{La}_{2-x}\text{Sr}_x\text{CuO}_4$  (LSCO) in Fig. 2], others observe an increase with doping [see data for  $\text{YBa}_2\text{Cu}_3\text{O}_{7-\delta}$  (YBCO) and  $\text{Bi}_2\text{Sr}_2\text{CaCu}_2\text{O}_{8+\delta}$  (Bi2212) in Fig. 2]. Within RMFT, we also verify that the nodal properties remain essentially unchanged when  $\Delta$  is set to 0; i.e., the doping dependence of  $v_F$  results from the vicinity of the state to a Mott insulator, rather than the occurrence of superconductivity itself.

We now calculate the spectral weight of the Gutzwiller-Bogoliubov quasiparticle (QP). The variational excited state in a projected superconductor is given by  $\exp(iS)|\Psi_k^-\rangle \equiv \exp(iS)P\gamma_{-k\uparrow}^\dagger|\Psi_0\rangle$ , where the corresponding Bogoliubov QP operator is defined by  $\gamma_{-k\uparrow}^\dagger \equiv u_k c_{-k\uparrow}^\dagger + v_k c_{k\uparrow}$ . In ARPES, the spectral weight corresponding to this excitation is determined by the matrix element  $M_k^- \equiv \langle \Psi_k^- | \tilde{c}_{k\uparrow} | \Psi \rangle / (N_k^- N_G)$ , where  $N_k^-$  and  $N_G$  are the norms of  $|\Psi_k^-\rangle$  and  $|\Psi\rangle$ , respectively. Here  $\tilde{c}_{k,\sigma} = \exp(-iS)c_{k,\sigma}\exp(iS)$ . Using the Gutzwiller renormalization scheme, we find  $M_k^- \approx Z_k n_{k\sigma}^0 + \mathcal{O}(t/U)^2$  [20] and

$$Z_k \approx g_t + \frac{g_3}{U} \left( \frac{1-x^2}{2} \epsilon_k^0 + \frac{3-x}{L} \sum_{k'} v_{k'}^2 \epsilon_{k'}^0 \right) \quad (4)$$

for the QP renormalization [21], with  $\epsilon_k^0 = 2t(\cos k_x + \cos k_y) + 4t' \cos k_x \cos k_y$ . Here  $n_{k\sigma}^0 = v_k^2$  is the momentum distribution in the unprojected wave function  $|\Psi_0\rangle$ . The renormalization  $Z_k$  of the nodal QP weight is plotted as a

$$n_{k\sigma}^{\text{inc}} \approx \frac{(1-x)^2}{2(1+x)} + \sum_{\tau} \frac{t_{\tau}}{2U} \cos(k\tau) \left[ \frac{(1-x)^3}{1+x} + \left( \frac{3g_s}{2} + 1 - g_3 \frac{3+x}{2} \right) |\Delta_{\tau}|^2 + \left( \frac{3g_s-1}{2} - g_3 \frac{3-x}{2} \right) \xi_{\tau}^2 \right], \quad (5)$$

which is a smooth function of  $k$ . Results are shown in Fig. 3(c). The incoherent weight is spread over the entire Brillouin zone and overlies the coherent part from the Gutzwiller-Bogoliubov quasiparticles. At half-filling, all weight becomes incoherent.

Finally, we consider the coherent QP weight  $M_k^- \approx Z_k v_k^2$  at the antinodal point  $\mathbf{k} = (\pi, 0)$ . As seen in Figs. 3(b) and 4, it exhibits a nonmonotonic behavior as a function of doping. Within our theory, this effect arises

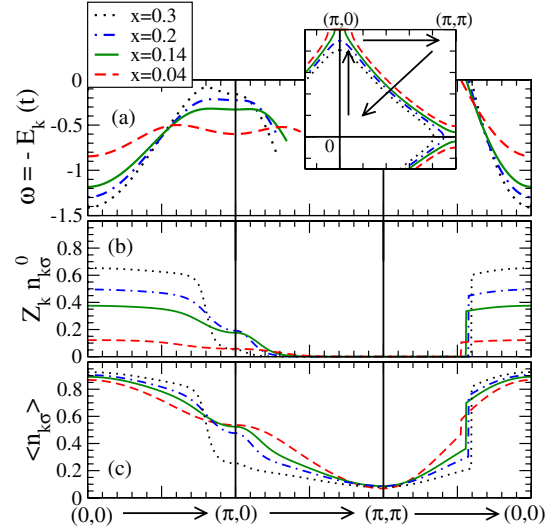


FIG. 3 (color online). (a) Energy dispersion  $\omega = -E_k$ , (b) quasiparticle weight  $Z_k n_{k\sigma}^0$ , and (c) momentum distribution  $\langle n_{k\sigma} \rangle$  of the Gutzwiller-Bogoliubov quasiparticle for different doping  $x$ ; the energy dispersion [in (a)] is shown only when the corresponding quasiparticle weight is finite [see (b)]. The corresponding Fermi surface  $\zeta_k = 0$  is shown in the inset in (a).

solid line in Fig. 2(b) and agrees well with VMC results [3]. The dashed lines correspond to results without  $t/U$  corrections. The dotted line  $Z_k = x$  is the result from slave boson mean field theory (SBMFT).

As a qualitative comparison with ARPES, we show the energy dispersion  $\omega = -E_k$  of the Gutzwiller-Bogoliubov QP along the directions  $(0, 0) \rightarrow (\pi, 0)$ ,  $(\pi, 0) \rightarrow (\pi, \pi)$ , and  $(\pi, \pi) \rightarrow (0, 0)$  for different  $x$  in Fig. 3. We emphasize that our calculations describe the low energy sector and do not seek to explain the “kink” at higher energies [19].

The spectral weight of the coherent peak, measured in ARPES, is related to the QP weight  $M_k^- \approx Z_k n_{k\sigma}^0$ ; it is shown in Fig. 3(b). As seen in the figure, the QP spectral weight is severely modified by Gutzwiller projection. It decreases with doping and vanishes at half-filling. This causes a shift of spectral weight to an incoherent background as seen in the momentum distribution function  $\langle n_{k\sigma} \rangle \approx Z_k v_k^2 + n_{k\sigma}^{\text{inc}} + \mathcal{O}(t/U)^2$ . While the first term corresponds to the coherent QP weight, the second gives the distribution of the incoherent part. We get

from a combination of the effects due to Gutzwiller projection and the topology change [see inset in Fig. 3(a)] of the underlying Fermi surface (FS). Figure 4(a) illustrates this clearly. While the QP weight renormalization  $Z_k$  increases with increasing doping,  $n_k^0 = v_k^2$  decreases due to the topology change, which occurs at  $x \approx 0.15-0.20$  for our choice of hopping parameters ( $t' = -t/4$ ). The change of the FS seems to be a generic feature of hole doped cuprates [22], although the exact doping concentration  $x$ ,

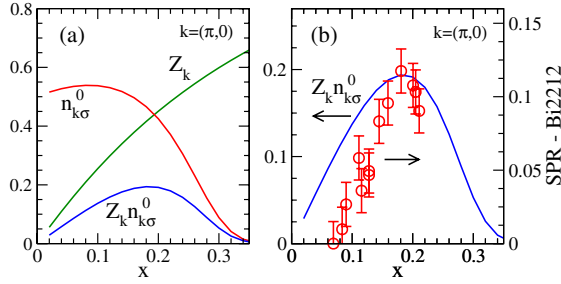


FIG. 4 (color online). Doping dependence at the antinodal point  $\mathbf{k} = (\pi, 0)$ : (a) QP renormalization  $Z_k$ , the unrenormalized QP weight  $n_{k\sigma}^0 = v_k^2$ , and the renormalized coherent QP weight  $Z_k n_{k\sigma}^0$ ; (b) coherent weight  $Z_k v_k^2$  compared with the experimentally determined SPR for Bi2212 [23].

for which this occurs, is sensitive to the ratio between various hopping parameters. The combined effect of strong correlations and topology change leads to a maximum of the QP weight for the doping level  $x$ , at which the underlying FS changes topology. This result should be tested by appropriate analyses of recent ARPES data [22]. Indications for such a behavior have already been published [23,24]. Feng *et al.* [23] extracted the superconducting peak ratio [SPR, illustrated in Fig. 4(b)], which is proportional to the coherent QP spectral weight  $Z_k v_k^2$ . They found that the SPR increases with small  $x$  and attains a maximum value around  $x \approx 0.2$ , where it begins to decrease. Ding *et al.* [24] reported similar results from ARPES. Although the topology change does not influence the stability of the SC state within RMFT, the SC pairing parameter  $\Phi$  (related to  $T_c$ ) and the QP weight  $Z_k v_k^2$  show some similarity as a function of doping.

To summarize, we studied the electronic structure of a Gutzwiller projected  $d$ -wave superconductor. A systematic combination of renormalized mean field theory and direct evaluation of matrix elements was applied to the Hubbard model in the strong coupling limit. Our analytical results can be used to fit experimentally observed quantities as well as those obtained from numerical methods. The dispersion of the Gutzwiller projected superconductor is renormalized in the vicinity of the Mott insulator, but the nodal Fermi velocity stays finite as the insulating limit is approached. The spectral weight of the nodal quasiparticle increases with doping, whereas that of the antinodal excitation shows nonmonotonic behavior, when the underlying Fermi surface changes topology. Our results can be checked by experimental observations from ARPES of high-temperature superconductors, thus providing a way to study the applicability of projected wave functions to these systems. The method we use is also amenable to other extensions such as coupling to the lattice, antiferromagnetism, and long range interactions.

We thank T. Valla, P.D. Johnson, J. Fink, and A. A. Kordyuk for discussions. V.N.M. acknowledges partial support from the PSC-CUNY Research Program. B.E. thanks the Hermann Willkomm Stiftung for supporting

his stay in Princeton.

- [1] J. C. Campuzano, M. R. Norman, and M. Randeria, in *Physics of Conventional and Unconventional Superconductors* (Springer-Verlag, Berlin, 2004); cond-mat/0209476.
- [2] A. Damascelli, Z. X. Shen, and Z. Hussain, *Rev. Mod. Phys.* **75**, 473 (2003).
- [3] A. Paramekanti, M. Randeria, and N. Trivedi, *Phys. Rev. Lett.* **87**, 217002 (2001); *Phys. Rev. B* **70**, 054504 (2004).
- [4] M. Randeria *et al.*, *Phys. Rev. Lett.* **95**, 137001 (2005).
- [5] P. W. Anderson, *Science* **235**, 1196 (1987); G. Baskaran, Z. Zou, and P. W. Anderson, *Solid State Commun.* **63**, 973 (1987).
- [6] C. Gros, *Phys. Rev. B* **38**, 931 (1988); H. Yokoyama and H. Shiba, *J. Phys. Soc. Jpn.* **57**, 2482 (1988); H. Yokoyama and M. Ogata, *J. Phys. Soc. Jpn.* **65**, 3615 (1996); S. Sorella *et al.*, *Phys. Rev. Lett.* **88**, 117002 (2002).
- [7] F.-C. Zhang *et al.*, *Supercond. Sci. Technol.* **1**, 36 (1988).
- [8] S. Yunoki, E. Dagotto, and S. Sorella, *Phys. Rev. Lett.* **94**, 037001 (2005).
- [9] G. J. Chen *et al.*, *Phys. Rev. B* **42**, 2662 (1990); A. Himeda and M. Ogata, *Phys. Rev. B* **60**, R9935 (1999); C. T. Shih *et al.*, *Phys. Rev. B* **70**, 220502(R) (2004).
- [10] C. P. Nave, D. A. Ivanov, and P. A. Lee, *Phys. Rev. B* **73**, 104502 (2006).
- [11] N. Fukushima *et al.*, *Phys. Rev. B* **72**, 144505 (2005).
- [12] This set of parameters has been widely used in the literature; e.g., E. Dagotto, *Rev. Mod. Phys.* **66**, 763 (1994).
- [13] C. Gros, R. Joynt, and T. M. Rice, *Phys. Rev. B* **36**, 381 (1987).
- [14] B. Edegger *et al.*, *Phys. Rev. B* **72**, 134504 (2005). See Appendix B for a derivation of the various Gutzwiller factors.
- [15] Several extensions to the Gutzwiller approximation have been proposed. See, e.g., M. Ogata and A. Himeda, *J. Phys. Soc. Jpn.* **72**, 374 (2003); G. Seibold and J. Lorenzana, *Phys. Rev. Lett.* **86**, 2605 (2001); J. Bünemann *et al.*, in *Frontiers in Magnetic Materials* (Springer-Verlag, Berlin, 2005).
- [16] Since the calculation of the expectation value  $\langle \tilde{H}_{\text{eff}} \rangle_0$  can be found in Ref. [14], and the derivation of the gap equations follows Ref. [7], we omit details here.
- [17] G. Kotliar and J. Liu, *Phys. Rev. B* **38**, 5142 (1988).
- [18] P. W. Anderson, *J. Phys. Chem. Solids* **63**, 2145 (2002).
- [19] P. V. Bogdanov *et al.*, *Phys. Rev. Lett.* **85**, 2581 (2000); P. D. Johnson *et al.*, *Phys. Rev. Lett.* **87**, 177007 (2001); X. J. Zhou *et al.*, *Nature (London)* **423**, 398 (2003); A. A. Kordyuk *et al.*, *Phys. Rev. B* **71**, 214513 (2005); A. A. Kordyuk (private communication); S. V. Borisenko *et al.*, *Phys. Rev. Lett.* **96**, 117004 (2006).
- [20] Here we dropped a small contribution to  $M_{\bar{k}}^-$  of  $\mathcal{O}(t/U)$ , which cannot be written as  $Z_k n_{k\sigma}^0$ .
- [21] A similar result with minor discrepancies was obtained independently in Ref. [4].
- [22] A. Kaminski *et al.*, cond-mat/0507106; T. Yoshida *et al.*, cond-mat/0510608.
- [23] D. L. Feng *et al.*, *Science* **289**, 277 (2000).
- [24] H. Ding *et al.*, *Phys. Rev. Lett.* **87**, 227001 (2001).